



Arylsulfanyl pyrazolones block mutant SOD1-G93A aggregation. Potential application for the treatment of amyotrophic lateral sclerosis

Tian Chen^a, Radhia Benmohamed^b, Anthony C. Arvanites^b, Hantamalala Ralay Ranaivo^{a,b,c,d,e,f,g}, Richard I. Morimoto^d, Robert J. Ferrante^{e,f}, D. Martin Watterson^c, Donald R. Kirsch^b, Richard B. Silverman^{a,g,*}

^a Department of Chemistry, Northwestern University, Evanston, IL 60208-3113, USA

^b Cambria Pharmaceuticals, Cambridge, MA 02142, USA

^c Center for Molecular Innovation and Drug Discovery, Northwestern University, Evanston, IL 60208-3113, USA

^d Department of Molecular Biosciences, Rice Institute for Biomedical Research, Northwestern University, Evanston, IL 60208-3500, USA

^e Geriatric Research Education and Clinical Center, Bedford Veterans Administration Medical Center, Bedford, MA 01730, USA

^f Department of Neurology, Laboratory Medicine and Pathology, and Psychiatry, Boston University School of Medicine, Boston, MA 02118, USA

^g Department of Molecular Biosciences, Chemistry of Life Processes Institute, Center for Molecular Innovation and Drug Discovery, Northwestern University, Evanston, IL 60208-3113, USA

ARTICLE INFO

Article history:

Received 11 September 2010

Revised 21 October 2010

Accepted 25 October 2010

Available online 30 October 2010

Keywords:

Arylsulfanyl pyrazolone

Amyotrophic lateral sclerosis

Mutant G93A SOD1

Blood–brain barrier penetration

ABSTRACT

Amyotrophic lateral sclerosis (ALS) is an orphan neurodegenerative disease currently without a cure. Mutations in copper/zinc superoxide dismutase 1 (SOD1) have been implicated in the pathophysiology of this disease. Using a high-throughput screening assay expressing mutant G93A SOD1, two bioactive chemical hit compounds (**1** and **2**), identified as arylsulfanyl pyrazolones, were identified. The structural optimization of this scaffold led to the generation of a more potent analogue (**19**) with an EC₅₀ of 170 nM. To determine the suitability of this class of compounds for further optimization, **1** was subjected to a battery of pharmacokinetic assays; most of the properties of **1** were good for a screening hit, except it had a relatively rapid clearance and short microsomal half-life stability. Compound **2** was found to be blood–brain barrier penetrating with a brain/plasma ratio = 0.19. The optimization of this class of compounds could produce novel therapeutic candidates for ALS patients.

© 2010 Elsevier Ltd. All rights reserved.

1. Introduction

Amyotrophic lateral sclerosis (ALS), also referred to as Lou Gehrig's disease, is a neurodegenerative disease defined by both upper and lower motor neuron death, with an inexorable progression towards death within 2–5 years from diagnosis.^{1–4} The incidence of ALS is ~1–2/100,000/year and may be rising. Currently, there is no effective treatment for this progressive fatal disorder. Riluzole, the only FDA approved drug for the treatment of ALS, prolongs the patient life by only two to three months.⁵ Therefore, there is an urgent need to develop new therapies for this lethal neurodegenerative disease.

Although 10% of ALS cases are familial (FALS), the clinical and pathological features of familial and sporadic ALS are similar. This has led to a strategy using FALS mutations for elucidating disease pathogenesis and identifying potential therapeutic targets for both forms of the disease.⁶ Modern genetics has identified mutations in Cu/Zn superoxide dismutase 1 (SOD1) that are responsible for

about 20% of the FALS patients.^{7,8} Recent studies show that mutations of the TAR DNA binding protein (TDP-43)⁹ and the fused in sarcoma/translated in liposarcoma (FUS/TLS) gene¹⁰ also cause FALS, but at much lower percentiles than SOD1 mutations. Interestingly, abnormal TDP-43 is *not* present in patients with mutant SOD1 FALS, yet it is present in sporadic ALS. While the exact pathophysiological mechanisms remain unclear in sporadic ALS, it has been postulated that oxidative stress, mitochondrial impairment, glutamate excitotoxicity, defective RNA processing and transport, and aberrant protein misfolding/aggregation may lead to increasingly fragile spinal cord and cell death.¹ Among these hypotheses, there is strong evidence that toxic aberrant protein misfolding/aggregation may trigger motor neuron dysfunction and cell death. Furthermore, mutant G93A SOD1 has been shown to form a distinct class of aggregated structures in PC12 cells destined for neuronal cell death.¹¹

This PC12 cell line was previously utilized in a high-throughput screen (HTS) as a cellular model of ALS,¹² which identified active compounds in the cytotoxicity assay. G93A SOD1 aggregation was cytotoxic, and inhibition of aggregation was cytoprotective. The percentage of cell survival was determined from the maximum

* Corresponding author. Tel.: +1 847 491 5663; fax: +1 847 491 7713.

E-mail address: Agman@chem.northwestern.edu (R.B. Silverman).

cell viability after exposure of test compounds to G93A SOD1 aberrant protein misfolding and aggregation. The EC_{50} values were also determined in the protection assay from the decrease in the toxic effects of mSOD1-G93A-YFP aggregation by the treatment of test compounds. From the HTS of a 50,000-member small molecule library, arylsulfanyl pyrazolone (ASP) compounds were identified as active (Fig. 1). The hit compounds showed 100% efficacy (cell viability) compared with the positive control (radicicol, 85% efficacy) in the cytotoxicity protection assay. The most potent hit compounds produced EC_{50} values between 400 nM and 15 μ M in the cytotoxicity protection assay (see Supplementary data). There were two distinguishing types of ASP compounds recognized from the HTS assay. Type I ASPs (Fig. 1) are 4-ethylidene-1*H*-pyrazol-5(4*H*)-ones with an alkene substituent on the pyrazolone ring; type II ASPs are 1*H*-pyrazol-3(2*H*)-ones. To initiate our optimization for this ASP scaffold, we designed and synthesized 17 ASP analogues (compound 3–19) to obtain preliminary structure–activity relationships (SAR) based on the ASP hits from the original HTS cellular model. Late drug attrition resulting from unsatisfactory pharmacokinetic (PK) profiles in clinical development has been recognized as a serious problem in the pharmaceutical industry.^{13,14} Therefore, early pharmacological property assessment is crucial to successful drug development and to direct the medicinal chemistry optimization.¹⁵

While we were initiating our SAR for the potency of the ASP scaffold, we also evaluated the PK potential of this scaffold as a central nervous system (CNS) drug. Drugs targeting CNS disorders must penetrate the blood–brain barrier (BBB) to be effective; statistics show that only about 2% of potential CNS compounds can penetrate the BBB, which contributes largely to the high failure rate of CNS drug candidates.^{16,17} To be a good drug candidate for the treatment of ALS, ASP derivatives must be able to demonstrate BBB permeability besides a good PK profile.¹⁸ Thus, a brain uptake study was performed as part of our early PK profile assessment of the ASP scaffold. Here we describe our efforts to improve the

potency and to determine in vitro pharmacokinetic properties and ability to cross the blood–brain barrier for this ASP scaffold.

2. Results and discussion

2.1. Chemistry

The synthesis of type I ASP compounds is outlined in Scheme 1. Furandione **20** was prepared by an acid-catalyzed aldol condensation from β -tetronic acid.¹⁹ Pyrazolone **21** was synthesized by refluxing dione **20** with hydrazine.²⁰ The resulting alcohol (**21**) was treated with PBr_3 to give **22**; substitution of the bromine atom with thiophenol afforded **3**. The synthesis of type II ASP compounds is outlined in Scheme 2. β -Ketoester **23** was prepared from ethyl 4-chloroacetoacetate and thiophenol,²¹ which was treated with hydrazine to give **5**.

2.2. Mutant SOD1-induced cytotoxicity protection assay

All of the ASP analogues showed 100% viability in the cytotoxicity protection assay. Based on the original ASP hits, a pyrazolone moiety is essential for activity in this scaffold (for a comparison of **513** with other hits see Supplementary data); therefore, the later designed analogues contained a pyrazolone moiety. Heteroatom-substituted aryl groups decreased the potency (see Supplementary data); therefore, newer designed ASP derivatives only included simple aryl substitution groups. Type I compound **3** showed an EC_{50} value over 32 μ M (Table 1), which is much less potent than the corresponding type II compound **4** (EC_{50} = 10.1 μ M). This is consistent with our observation that, in general, type I hits were not as potent as type II hits (see Supplementary data). Therefore, SAR studies focused on type II ASPs. To explore the effect of substitution on the aryl ring in the ASP scaffold, a chlorine atom was substituted at position 4. Compound **5** (Table 1) was significantly more potent than unsubstituted analogue **4**. An SAR was developed by replacement of the 4-chlorine with other electron-withdrawing groups, electron-donating groups, and substituents with varying sizes. Except for the very large phenyl or small fluorine, changes in electron-withdrawing or electron-donating groups did not have a significant effect on EC_{50} . To determine the effect of substitution on the pyrazolone ring, type II ASP analogues having an *N*(2)-methyl and *N*(2)-benzyl substituent (**6** and **7**) were prepared by the synthetic route described in Scheme 2 using methylhydrazine and phenylhydrazine, respectively, instead of hydrazine. Neither of these analogues was as potent as **5**, the corresponding unsubstituted pyrazolone analogue (Table 1).

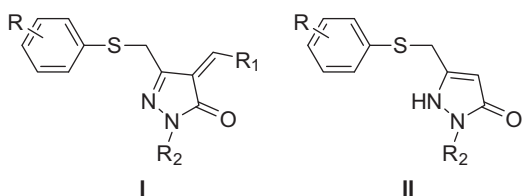
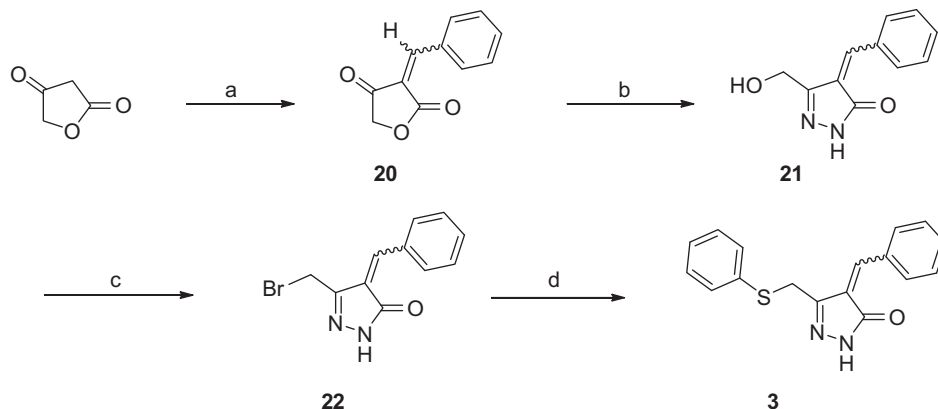
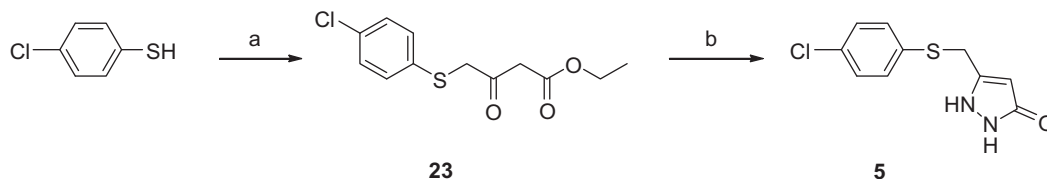


Figure 1. ASP HTS hits. R_1 , alkyl or substituted aromatic groups; R_2 , proton or substituted aromatic groups; R , various alkyl and/or halogen groups.



Scheme 1. Reagents and conditions: (a) benzaldehyde, HCl, room temperature, 5 min, 48%; (b) NH_2NH_2 , EtOH, reflux, 1 h, 28%; (c) PBr_3 , THF, room temperature, 6 h, 41%; (d) benzenethiol, K_2CO_3 , DMF, 70 $^\circ$ C, 18 h, 27%.



Scheme 2. Reagents and conditions: (a) ethyl 4-chloroacetoacetate, Et₃N, DCM, 0 °C, 30 min, 96%; (b) NH₂NH₂, EtOH, room temperature, overnight, 72%.

Table 1
SAR of selected ASPs^a

ID	R ₁	R ₂	EC ₅₀ (μM)
3	—	—	>32
4	H	H	10.11
5	Cl	H	1.93
6	Cl	Me	5.4
7	Cl	Ph	3.46
8	<i>t</i> -Bu	H	2.31
9	NO ₂	H	2.40
10	MeO	H	1.81
11	Ph	H	4.06
12	F	H	3.44
13	Br	H	1.80

^a Average Z' factor value = 0.5.

The two most potent hit compounds in the type I and type II series (**1** and **2**) were 2,4-dichloro-5-methyl- and 4-chloro-2,5-dimethyl-substituted on their phenyl rings, respectively. The methyl substituents could be metabolized by CYP isozymes.²² In addition, these substituents are lipophilic, which also may lead to unsatisfactory pharmacokinetic profiles. Therefore, we synthesized (Scheme 2) and examined a series of monochloro- and dichloro-phenyl-substituted ASP analogues (Table 2). 3-Chloro substituted analogue **15** was more potent than the 2-chloro substituted one (**14**). Di-chloro substituted analogues were found to be as good or better than monochloro substituted ones; **19** had an EC₅₀ value of 170 nM, more than twice the potency of **2**.

2.3. In vitro ADME studies

Because of the importance of pharmacokinetic properties of potential drug molecules, in vitro ADME studies, including aqueous solubility, Caco-2 monolayer permeability, PBS/mouse plasma stability, and human and mouse microsomal stability, were carried out to identify the PK profiles of this scaffold at an early stage of our hit-to-lead optimization. The representative compound tested was **1**, the second most potent ASP hit from the original HTS. Results are summarized in Table 3.

To mimic the conditions typically used in our in vitro cell-based HTS assays, the aqueous solubility of **1** was evaluated by diluting it from a stock solution in DMSO to a final concentration of 1% DMSO in PBS. The maximum solubility was considered to be the highest concentration that showed no precipitation. Compound **1** was found to have a moderate level of aqueous solubility²³ (56 μM; 16.4 μg/mL).

Compound **1** had moderate permeability²⁴ in the Caco-2 permeability assay (P_{app} (A→B) = 4.7×10^{-6} cm/s). The permeability through Caco-2 monolayer cells has been correlated with in vivo

Table 2
SAR of type II ASPs with a monochloro- or dichloro-aryl substituent^a

ID	R	EC ₅₀ (μM)
1	2,4-Dichloro-5-methyl	0.55
2	2,5-Dimethyl-4-chloro	0.40
14	2-Chloro-	3.05
15	3-Chloro-	1.11
16	2,4-Dichloro-	1.15
17	3,4-Dichloro-	1.89
18	2,6-Dichloro-	0.95
19	3,5-Dichloro-	0.17

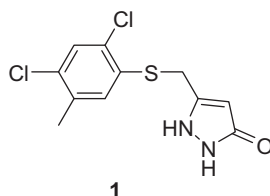
^a Average Z' factor value = 0.5.

intestinal permeability.²⁵ The low efflux ratio (P_{app} (B→A)/ P_{app} (A→B) = 0.1) bodes well for CNS applications.

Human and mouse microsomal stability of **1** was tested at 5 μM at 37 °C for 1 h. Compound **1** shows rapid clearance²⁶ (58.5 mL/min/kg) and relatively short metabolic half-life ($T_{1/2}$ = 39 min) with human liver microsomes. As is typically observed, mouse liver microsome stability was even lower; **1** was rapidly cleared (292 mL/min/kg) and metabolized ($T_{1/2}$ = 13 min) by mouse liver microsomes. Compound **1** also showed moderate metabolism²⁶ in the absence of NADPH, which might result from non-NADPH dependent metabolic pathways; its stability in PBS was excellent. The stability of **1** in mouse plasma was evaluated by incubating 5 μM compound with mouse plasma at 37 °C for 1 h. Compound **1** shows low metabolic stability in mouse plasma ($T_{1/2}$ = 16 min). Overall, this scaffold has good potency, but is not very metabolically stable.

2.4. Brain penetration of **2**

The most potent ASP hit compound (**2**) was tested for its ability to cross the blood–brain barrier. Compound **1**, a close structural relative of **2**, was selected as the internal standard for **2** in this study. A known amount of the internal standard (**1**) was added prior to extraction, and the final quantification was obtained as a ratio of compound **2–1** by LC–MS/MS. Standard curves for the concentration of **2** in both plasma and brain are included in Supplementary data. Three mice were dosed intraperitoneally (ip) with **2** at 1 mg/kg. Similar to **1**, compound **2** was found to have low metabolic stability in mouse ($T_{1/2}$ = 15 min; see Supplementary data). Therefore, the mice were sacrificed 10 min after administration, while the clearance of **2** was still less than 50%. The concentration of **2** was calculated in μg/mL in plasma, and in μg/g in brain. To directly compare the amount of **2** in plasma and brain, both of the values were converted to μM; the density of brain was assumed to be 1.0 g/mL.^{27,28} The brain/plasma ratio of **2** at 1 mg/kg after 10 min of ip administration was about 0.19 (Table

Table 3
In vitro pharmacokinetic assays of **1**

Aqueous solubility	Maximum solubility (μM)		
	56		
Caco-2 permeability	P_{app} (A→B) (10^{-6} cm/s)	P_{app} (B→A) (10^{-6} cm/s)	Ratio (B→A/A→B)
	4.7	0.46	0.1
PBS/mouse plasma stability	Plasma $T_{1/2}$ (min)	PBS amount remaining at 60 min (%)	Recovery plasma versus PBS (%)
	16	100	91
Microsomal stability (human)	CL'_{int} (mL/min/kg)	$T_{1/2}$ (min)	CL'_{int} no NADPH (mL/min/kg)
	58.5	39	16.2
Microsomal stability (mouse)	292	13	61.2

4), indicating that the ASP scaffold is capable of permeation into the brain, but not highly efficiently.

3. Conclusion

In summary, a new chemical scaffold has been identified from a previously reported HTS cellular model targeting familial ALS. Inspired from the original ASP hits, a SAR study led to the generation of a new ASP compound (**19**) with improved in vitro potency of 170 nM. In vitro pharmacokinetics were carried out, and the in vivo brain/plasma ratio was determined for two ASP hit compounds (**1** and **2**, respectively). It appears that this scaffold needs to be modified to protect it from microsomal and plasma enzymes. The most likely site of metabolism is the sulfide sulfur atom, which should be susceptible to P450 oxidation.

4. Experimental section

4.1. Chemistry

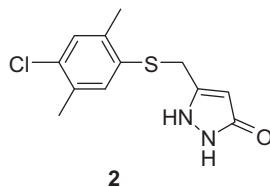
4.1.1. General methods

All reagents were purchased from Aldrich, Alfa Aesar, Oakwood Inc., and Maybridge Ltd. They were used without further purification unless stated otherwise. Tetrahydrofuran was distilled under nitrogen from sodium/benzophenone. Thin-layer chromatography was carried out on E. Merck precoated Silica Gel 60 F₂₅₄ plates. Compounds were visualized with ferric chloride reagent or a UV lamp. Column chromatography was performed with E. Merck Silica Gel 60 (230–400 mesh). Proton nuclear magnetic resonances (¹H NMR) were recorded in deuterated solvents on a Varian Inova 400 (400 MHz), a Varian Inova 500 (500 MHz) and a Bruker

Ag500 (500 MHz) spectrometer. Chemical shifts are reported in parts per million (ppm, δ) using various solvents as internal standards (CDCl₃, δ 7.26 ppm; DMSO-*d*₆, δ 2.50 ppm). ¹H NMR splitting patterns are designated as singlet (s), doublet (d), triplet (t), or quartet (q). Splitting patterns that could not be interpreted or easily visualized were recorded as multiplet (m) or broad (br). Coupling constants are reported in Hertz (Hz). Proton-decoupled carbon (¹³C NMR) spectra were recorded on a Varian Inova 500, a Varian Inova 400, and a Bruker Ag500 (125.7, 100.6, and 125.7 MHz, respectively) spectrometer and are reported in ppm using various solvents as internal standards (CDCl₃, δ 77.23 ppm; DMSO-*d*₆, δ 39.52 ppm). Electrospray mass spectra (ESMS) were obtained using an LCQ-Advantage with methanol as the solvent in the positive ion mode. High-resolution mass spectra were carried out using a VG70-250SE mass spectrometer. All final compounds were analyzed for purity by HPLC using a Luna C18 (2) column (4.6 × 150, 5 μm ; Phenomenex, Torrance, CA) at a flow rate of 1 mL/min with multiple HPLC conditions. Sample elution was detected by absorbance at 254 nm. The HPLC was performed on a Beckman System Gold chromatograph (Model 125P solvent module and Model 166 detector).

4.1.2. 3-Benzylidene-furan-2,4(3H,5H)-dione (**20**)

Tetronic acid (300 mg, 3 mmol) was added to benzaldehyde (1.0 mL, 9 mmol), and the resulting solution was stirred. HCl (37.7%, 0.1 mL) was added dropwise. The reaction mixture was vigorously stirred until it solidified. The solid product was crushed, soaked in hexane and washed with hexane. The crude product was purified by recrystallization (ethyl acetate/hexanes = 8/2) to give compound **20** (0.27 g, 48%) as a yellow solid. ¹H NMR (500 MHz, CDCl₃, δ): 8.45 (m, 2H), 8.03 (s, 1H), 7.62 (m, 3H), 4.78 (s, 1H), 4.65 (s, 1H).

Table 4
Brain/plasma ratio of **2** at 1 mg/kg via ip administration^a

Time after administration	Brain concentration ($\mu\text{g/g}$)	Plasma concentration ($\mu\text{g/mL}$)	Brain/plasma ratio
10 min	0.36 ± 0.11	1.96 ± 0.87	0.19 ± 0.04

^a Mean value ± standard deviation, where appropriate.

4.1.3. 4-Benzylidene-3-(hydroxymethyl)-1H-pyrazol-5(4H)-one (21)

To a suspension of ethanol (2 mL) and **20** (367 mg, 2 mmol) was added an ethanolic solution of hydrazine (2 N, 1 mL). The resulting suspension was refluxed for 1 h, during which time all of the **20** dissolved, and a new precipitate formed. The resulting mixture was cooled in an ice-bath for 20 min. The white precipitate was filtered and washed with cold ethanol to give **21** (77 mg, 28%). ¹H NMR (500 MHz, CDCl₃, δ): 11.68 (br, 1H), 11.22 (br, 1H), 8.03 (s, 1H), 7.32–7.80 (m, 5H), 4.98 (s, 2H).

4.1.4. 4-Benzylidene-3-(bromomethyl)-1H-pyrazol-5(4H)-one (22)

PBr₃ (30 μL, 0.38 mmol) was added to a suspension of **21** (0.23 g, 1.1 mmol) in THF (5 mL) at 0 °C under N₂. The reaction mixture was warmed to room temperature after 5 min. Additional PBr₃ (30 μL, 0.38 mmol) was added after 1 h. The resulting suspension gradually became a solution and was stirred overnight. The reaction mixture was then quenched with brine, and the aqueous layer was extracted with CH₂Cl₂. The combined organic layer was washed with brine, dried over Na₂SO₄, and evaporated to dryness. Compound **22** (0.125 g, 41%) was obtained by flash column chromatography (ethyl acetate/hexanes = 1/4) as a yellow solid. ¹H NMR (500 MHz, CDCl₃, δ): 11.22 (br, 1H), 8.03 (s, 1H), 7.32–7.80 (m, 5H), 4.98 (s, 2H).

4.1.5. 4-Benzylidene-3-(phenylthiomethyl)-1H-pyrazol-5(4H)-one (3)

Benzenethiol (61 μL, 0.60 mmol) was added to a suspension of **22** (0.13 g, 0.50 mmol) and anhydrous potassium carbonate (0.42 g, 3.0 mmol) in DMF (2 mL) at room temperature. The reaction temperature was gently brought to 70 °C. After the resulting suspension was stirred for 18 h, the reaction mixture was quenched with HCl (0.25 N), and the aqueous layer was extracted with EtOAc. The combined organic layer was washed with brine, dried over Na₂SO₄, and evaporated to dryness. Compound **3** (40 mg, 27%) was obtained by flash column chromatography (ethyl acetate/hexanes = 1/2) as a white solid. ¹H NMR (500 MHz, DMSO-*d*₆, δ): 11.29 (s, 1H), 8.03 (s, 1H), 7.68–7.18 (m, 10H), 5.19 (dd, *J* = 32.0, 16.5 Hz, 2H); ¹³C NMR (125 MHz, DMSO-*d*₆, δ): 175.8, 161.8, 144.3, 133.9, 129.8, 128.8, 127.6, 126.9, 126.4, 125.5, 94.0, 66.3, 32.2; HPLC method A (isocratic; ACN/H₂O 80:20, 60 min; 0.1% TFA): *rt* = 7.12 min, purity = 91.8%; HPLC method B (isocratic; MeOH/H₂O 80:20, 60 min; 0.1% TFA): *rt* = 15.82 min, purity = 90.1%.

4.1.6. General procedure for ASPII products. 5-((4-Chlorophenylthio)methyl)-1H-pyrazol-3(2H)-one (5)

4-Chlorothiophenol (1.1 g, 7.61 mmol) was mixed with ethyl 4-chloroacetoacetate (0.95 mL, 7.00 mmol) in CH₂Cl₂ (100 mL) at 0 °C. Triethylamine (1.5 mL, 10.8 mmol) was then added dropwise. After the resulting suspension was stirred at 0 °C for another 30 min, the reaction mixture was poured into water, and the aqueous layer was extracted with EtOAc. The combined organic layer was washed with saturated NaHCO₃, HCl (0.25 N), brine, concentrated in vacuo, and purified by flash column chromatography (ethyl acetate/hexanes = 1/9) to afford **23** as a light yellow oil, which was not very stable. Therefore, **23** was used directly for the next step immediately after the flash column chromatography purification.

Compound **23** (0.48 g, 1.76 mmol) was stirred in EtOH (5 mL), and an ethanolic solution of NH₂NH₂ (2 N, 0.88 mL, 1.76 mmol) was added. The resulting solution was stirred overnight at room temperature, during which time a precipitate formed. The precipitate was filtered, washed with cold EtOH, and dried in vacuo to afford **5** (0.31 g, 69%, two steps) as a white solid. ¹H NMR (500 MHz, DMSO-*d*₆, δ): 11.55 (br s, 1H), 9.47 (br s, 1H), 7.36 (s, 4H), 5.31 (s,

1H), 4.08 (s, 2H); ¹³C NMR (125 MHz, DMSO-*d*₆, δ): 159.8, 140.6, 135.1, 130.6, 129.9, 128.9, 88.8, 28.1; HRMS (*m/z*): [M+H]⁺ calcd for C₁₀H₉ClN₂OS, 240.01241; found 240.01935; HPLC method A (isocratic; ACN/H₂O 30:70, 60 min; 0.1% TFA): *rt* = 12.42 min, purity = 97.1%; HPLC method B (isocratic; MeOH/H₂O 50:50, 60 min; 0.1% TFA): *rt* = 20.67 min, purity = 97.0%.

4.1.7. 5-((2,4-Dichloro-5-methylphenylthio)methyl)-1H-pyrazol-3(2H)-one (1)

Compound **1** was purchased from Maybridge Ltd, Trevillet, UK; ¹H NMR (500 MHz, DMSO-*d*₆, δ): 11.62 (br s, 1H), 9.72 (br s, 1H), 7.57 (s, 1H), 7.46 (s, 1H), 5.39 (s, 1H), 4.15 (s, 2H), 2.30 (s, 3H).

4.1.8. 5-((4-Chloro-2,5-dimethylphenylthio)methyl)-1H-pyrazol-3(2H)-one (2)

Compound **2** was purchased from Maybridge Ltd, Trevillet, UK; ¹H NMR (500 MHz, DMSO-*d*₆, δ): 11.56 (br, 1H), 9.47 (br, 1H), 7.32 (s, 1H), 7.26 (s, 1H), 5.33 (s, 1H), 4.05 (s, 2H), 2.27 (s, 3H), 2.19 (s, 3H).

4.1.9. 5-(Phenylthiomethyl)-1H-pyrazol-3(2H)-one (4)

In analogy to **5**, compound **4** was prepared following the general procedure of ASPII products. Benzenethiol (0.9 mL, 8.81 mmol) was treated with ethyl 4-chloroacetoacetate (1.20 mL, 8.81 mmol) and triethylamine (1.30 mL, 9.33 mmol) to afford ethyl 3-oxo-4-(phenylthio)butanoate (1.80 g, 7.54 mmol). Immediately after flash column chromatography, ethyl 3-oxo-4-(phenylthio)butanoate (0.53 g, 2.22 mmol) was treated with NH₂NH₂ (2 N in EtOH, 1.12 mL, 2.24 mmol) to give **4** as a white solid (0.36 g, 67%, two steps). ¹H NMR (500 MHz, DMSO-*d*₆, δ): 11.54 (br s, 1H), 9.55 (br s, 1H), 7.34–7.29 (m, 4H), 7.19 (t, *J* = 7.0 Hz, 1H), 5.31 (s, 1H), 4.07 (s, 2H); ¹³C NMR (125 MHz, DMSO-*d*₆, δ): 160.1, 148.6, 140.5, 132.4, 128.0, 126.0, 88.9, 34.1, 31.0, 28.2; HRMS (*m/z*): [M+H]⁺ calcd for C₁₀H₁₀N₂OS, 207.0587; found 207.0586; HPLC method A (gradient; ACN/H₂O 0:100–80:20, 0–30 min, ACN/H₂O 80:20–0:100, 30–60 min; 0.1% TFA): *rt* = 17.0 min, purity = 99.3%; HPLC method B (isocratic; MeOH/H₂O 50:50, 60 min; 0.1% TFA): *rt* = 6.67 min, purity = 95.7%.

4.1.10. 5-((4-Chlorophenylthio)methyl)-2-methyl-1H-pyrazol-3(2H)-one (6)

In analogy to **5**, compound **6** was prepared following the general procedure of ASPII products. 4-Chlorobenzenethiol (1.1 g, 7.61 mmol) was treated with ethyl 4-chloroacetoacetate (0.95 mL, 7.00 mmol) and triethylamine (1.50 mL, 10.8 mmol) to afford **23** (1.82 g, 6.67 mmol). Immediately after flash column chromatography, **23** (0.70 g, 2.58 mmol) was allowed to react with methylhydrazine (2 N in EtOH, 1.30 mL, 2.60 mmol) to give **6** as a white solid (0.10 g, 14%, two steps). ¹H NMR (500 MHz, DMSO-*d*₆, δ): 10.88 (br s, 1H), 7.35 (s, 4H), 5.24 (s, 1H), 3.99 (s, 2H), 3.43 (s, 3H); ¹³C NMR (125 MHz, DMSO-*d*₆, δ): 152.5, 145.4, 136.0, 129.3, 128.8, 85.2, 33.0, 30.6; HPLC method A (gradient; ACN/H₂O 30:70–80:20, 0–20 min, ACN/H₂O 80:20–30:70, 20–40 min; 0.1% TFA): *rt* = 9.33 min, purity = 99.0%; HPLC method B (isocratic; MeOH/H₂O 50:50, 60 min; 0.1% TFA): *rt* = 16.72 min, purity = 99.1%.

4.1.11. 5-((4-Chlorophenylthio)methyl)-2-phenyl-1H-pyrazol-3(2H)-one (7)

In analogy to **5**, compound **7** was prepared following the general procedure of ASPII products. 4-Chlorobenzenethiol (1.1 g, 7.61 mmol) was treated with ethyl 4-chloroacetoacetate (0.95 mL, 7.00 mmol) and triethylamine (1.50 mL, 10.8 mmol) to afford **23** (1.82 g, 6.67 mmol). Immediately after flash column chromatography, **23** (0.58 g, 2.13 mmol) was allowed to react with phenylhydrazine (2 N in EtOH, 1.06 mL, 2.12 mmol) to give **7** as a white solid (0.11 g, 10%, two steps). ¹H NMR (500 MHz,

DMSO- d_6 , δ): 11.67 (br s, 1H), 7.67 (d, $J = 8.5$ Hz, 2H), 7.45–7.36 (m, 6H), 7.24 (t, $J = 7.5$ Hz, 1H), 5.46 (s, 1H), 4.11 (s, 2H); ^{13}C NMR (125 MHz, DMSO- d_6 , δ): 153.1, 148.2, 138.6, 135.5, 130.2, 129.5, 128.9, 128.8, 125.5, 120.9, 87.0, 25.1; HPLC method A (gradient; ACN/H₂O 30:70–80:20, 0–20 min, ACN/H₂O 80:20–30:70, 20–40 min; 0.1% TFA): $r_t = 18.88$ min, purity = 96.4%; HPLC method B (isocratic; MeOH/H₂O 70:30, 60 min; 0.1% TFA): $r_t = 12.98$ min, purity = 96.0%.

4.1.12. 5-((4-*tert*-Butylphenylthio)methyl)-1H-pyrazol-3(2H)-one (8)

In analogy to **5**, compound **8** was prepared following the general procedure of ASPII products. 4-*tert*-Butylbenzenethiol (1.04 mL, 6.01 mmol) was treated with ethyl 4-chloroacetoacetate (0.82 mL, 6.02 mmol) and triethylamine (1.26 mL, 9.01 mmol) to afford ethyl 4-(4-*tert*-butylphenylthio)-3-oxobutanoate (1.65 g, 5.60 mmol). Immediately after flash column chromatography, ethyl 4-(4-*tert*-butylphenylthio)-3-oxobutanoate (1.09 g, 3.70 mmol) was allowed to react with hydrazine (2 N in EtOH, 1.86 mL, 3.72 mmol) to give **8** as a white solid (0.54 g, 51%, two steps). ^1H NMR (500 MHz, DMSO- d_6 , δ): 11.22 (br s, 1H), 10.07 (br s, 1H), 7.33–7.26 (m, 4H), 5.34 (s, 1H), 4.04 (s, 2H), 1.25 (s, 9H); ^{13}C NMR (125 MHz, DMSO- d_6 , δ): 160.1, 148.6, 140.6, 132.4, 128.0, 126.0, 88.9, 34.1, 31.0, 28.2; HPLC method A (gradient; ACN/H₂O 0:100–80:20, 0–30 min, ACN/H₂O 80:20–0:100, 30–60 min; 0.1% TFA): $r_t = 22.88$ min, purity = 96.9%; HPLC method B (isocratic; MeOH/H₂O 60:40, 60 min; 0.1% TFA): $r_t = 15.88$ min, purity = 98.8%.

4.1.13. 5-((4-Nitrophenylthio)methyl)-1H-pyrazol-3(2H)-one (9)

In analogy to **5**, compound **9** was prepared following the general procedure of ASPII products. 4-Nitrobenzenethiol (1.00 g, 6.44 mmol) was treated with ethyl 4-chloroacetoacetate (0.88 mL, 6.44 mmol) and triethylamine (1.35 mL, 9.67 mmol) to afford ethyl 4-(4-nitrophenylthio)-3-oxobutanoate (1.56 g, 5.52 mmol). Immediately after flash column chromatography ethyl 4-(4-nitrophenylthio)-3-oxobutanoate (1.04 g, 3.67 mmol) was allowed to react with hydrazine (2 N in EtOH, 2.07 mL, 4.14 mmol) to give **9** as a white solid (0.40 g, 33%, two steps). ^1H NMR (500 MHz, DMSO- d_6 , δ): 11.64 (br s, 1H), 9.52 (br s, 1H), 8.13 (d, $J = 8.5$ Hz, 2H), 7.55 (d, $J = 8.5$ Hz, 2H), 5.41 (s, 1H), 4.26 (s, 2H); ^{13}C NMR (125 MHz, DMSO- d_6 , δ): 161.0, 146.8, 144.6, 138.4, 126.4, 123.9, 90.2, 25.9; HPLC method A (isocratic; ACN/H₂O 25:75, 60 min; 0.1% TFA): $r_t = 14.85$ min, purity = 97.1%; HPLC method B (isocratic; MeOH/H₂O 50:50, 60 min; 0.1% TFA): $r_t = 9.98$ min, purity = 99.9%.

4.1.14. 5-((4-Methoxyphenylthio)methyl)-1H-pyrazol-3(2H)-one (10)

In analogy to **5**, compound **10** was prepared following the general procedure of ASPII products. 4-Methoxybenzenethiol (0.87 mL, 7.07 mmol) was treated with ethyl 4-chloroacetoacetate (0.97 mL, 7.12 mmol) and triethylamine (1.50 mL, 10.8 mmol) to afford ethyl 4-(4-methoxyphenylthio)-3-oxobutanoate (1.85 g, 6.89 mmol). Immediately after flash column chromatography ethyl 4-(4-methoxyphenylthio)-3-oxobutanoate (1.78 g, 6.63 mmol) was allowed to react with hydrazine (2 N in EtOH, 3.32 mL, 6.63 mmol) to give **10** as a white solid (0.34 g, 21%, two steps). ^1H NMR (500 MHz, DMSO- d_6 , δ): 11.45 (br s, 1H), 9.36 (br s, 1H), 7.29 (d, $J = 8.5$ Hz, 2H), 6.89 (d, $J = 9.0$ Hz, 2H), 5.22 (s, 1H), 3.93 (s, 2H), 3.73 (s, 3H); ^{13}C NMR (125 MHz, DMSO- d_6 , δ): 161.5, 158.5, 140.2, 132.3, 125.6, 114.7, 89.7, 55.2, 29.8; HPLC method A (isocratic; ACN/H₂O 40:60, 60 min; 0.1% TFA): $r_t = 5.55$ min, purity = 95.4%; HPLC method B (isocratic; MeOH/H₂O 50:50, 60 min; 0.1% TFA): $r_t = 7.65$ min, purity = 99.6%.

4.1.15. 5-((Biphenyl-4-ylthio)methyl)-1H-pyrazol-3(2H)-one (11)

In analogy to **5**, compound **11** was prepared following the general procedure of ASPII products. Biphenyl-4-thiol (0.50 g, 2.68 mmol) was treated with ethyl 4-chloroacetoacetate (0.37 mL, 2.68 mmol) and triethylamine (0.56 mL, 4.02 mmol) to afford ethyl 4-(biphenyl-4-ylthio)-3-oxobutanoate (0.72 g, 2.30 mmol). Immediately after flash column chromatography ethyl 4-(4-methoxyphenylthio)-3-oxobutanoate (1.78 g, 6.63 mmol) was allowed to react with hydrazine (2 N in EtOH, 1.15 mL, 2.30 mmol) to give **11** as a white solid (0.36 g, 47%, two steps). ^1H NMR (500 MHz, DMSO- d_6 , δ): 11.39 (br s, 1H), 9.52 (br s, 1H), 7.66–7.34 (m, 9H), 5.36 (s, 1H), 4.12 (s, 2H); ^{13}C NMR (125 MHz, DMSO- d_6 , δ): 161.0, 139.4, 137.6, 135.3, 129.0, 128.5, 127.5, 127.2, 126.5, 89.2, 27.8; HPLC method A (gradient; ACN/H₂O 30:70–80:20, 0–20 min, ACN/H₂O 80:20–30:70, 20–40 min; 0.1% TFA): $r_t = 11.62$ min, purity = 95.3%; HPLC method B (isocratic; MeOH/H₂O 60:40, 60 min; 0.1% TFA): $r_t = 13.55$ min, purity = 98.8%.

4.1.16. 5-((4-Fluorophenylthio)methyl)-1H-pyrazol-3(2H)-one (12)

In analogy to **5**, compound **12** was prepared following the general procedure of ASPII products. 4-Fluorobenzenethiol (0.84 mL, 7.80 mmol) was treated with ethyl 4-chloroacetoacetate (1.06 mL, 7.80 mmol) and triethylamine (1.63 mL, 11.7 mmol) to afford ethyl 4-(4-fluorophenylthio)-3-oxobutanoate (1.72 g, 7.67 mmol). Immediately after flash column ethyl 4-(4-fluorophenylthio)-3-oxobutanoate (1.72 g, 7.67 mmol) was allowed to react with hydrazine (2 N in EtOH, 4.00 mL, 8.00 mmol) to give **12** as a white solid (0.71 g, 40%, two steps). ^1H NMR (500 MHz, DMSO- d_6 , δ): 11.52 (br s, 1H), 9.40 (br s, 1H), 7.40–7.37 (m, 2H), 7.17 (t, $J = 8.8$ Hz, 2H), 5.27 (s, 1H), 4.03 (s, 1H); ^{13}C NMR (125 MHz, DMSO- d_6 , δ): 161.9, 160.0, 131.3, 116.1, 115.9, 89.4, 28.7; HPLC method A (gradient; ACN/H₂O 30:70–80:20, 0–20 min, ACN/H₂O 80:20–30:70, 20–40 min; 0.1% TFA): $r_t = 6.58$ min, purity = 98.8%; HPLC method B (isocratic; MeOH/H₂O 50:50, 60 min; 0.1% TFA): $r_t = 7.48$ min, purity = 99.5%.

4.1.17. 5-((4-Bromophenylthio)methyl)-1H-pyrazol-3(2H)-one (13)

In analogy to **5**, compound **13** was prepared following the general procedure of ASPII products. 4-Bromobenzenethiol (1.00 g, 5.29 mmol) was treated with ethyl 4-chloroacetoacetate (0.72 mL, 5.29 mmol) and triethylamine (1.11 mL, 7.93 mmol) to afford ethyl 4-(4-bromophenylthio)-3-oxobutanoate (1.56 g, 4.94 mmol). Immediately after flash column ethyl 4-(4-fluorophenylthio)-3-oxobutanoate (1.72 g, 7.67 mmol) was allowed to react with hydrazine (2 N in EtOH, 1.67 mL, 3.34 mmol) to give **13** as a white solid (0.69 g, 67%, two steps). ^1H NMR (500 MHz, DMSO- d_6 , δ): 11.45 (br s, 1H), 9.79 (br s, 1H), 7.48 (d, $J = 8.5$ Hz, 2H), 7.28 (d, $J = 8.5$ Hz, 2H), 5.32 (s, 1H), 4.08 (s, 2H); ^{13}C NMR (125 MHz, DMSO- d_6 , δ): 160.0, 140.6, 135.5, 131.7, 130.0, 118.8, 88.8, 27.9; HPLC method A (gradient; ACN/H₂O 30:70–80:20, 0–20 min, ACN/H₂O 80:20–30:70, 20–40 min; 0.1% TFA): $r_t = 8.88$ min, purity = 99.0%; HPLC method B (isocratic; MeOH/H₂O 50:50, 60 min; 0.1% TFA): $r_t = 15.72$ min, purity = 99.8%.

4.1.18. 5-((2-Chlorophenylthio)methyl)-1H-pyrazol-3(2H)-one (14)

In analogy to **5**, compound **14** was prepared following the general procedure of ASPII products. 2-Chlorobenzenethiol (0.50 g, 3.46 mmol) was treated with ethyl 4-chloroacetoacetate (0.47 mL, 3.46 mmol) and triethylamine (0.72 mL, 5.19 mmol) to afford ethyl 4-(2-chlorophenylthio)-3-oxobutanoate (0.96 g, 3.46 mmol). Immediately after flash column ethyl 4-(2-chlorophenylthio)-3-oxobutanoate (0.96 g, 3.46 mmol) was allowed to react with hydrazine

(2 N in EtOH, 1.76 mL, 3.52 mmol) to give **14** as a white solid (0.41 g, 48%, two steps). ¹H NMR (500 MHz, DMSO-*d*₆, δ): 11.60 (br s, 1H), 9.54 (br s, 1H), 7.46–7.17 (m, 4H), 5.39 (s, 1H), 4.14 (s, 2H); ¹³C NMR (125 MHz, DMSO-*d*₆, δ): 161.2, 138.2, 135.5, 130.7, 129.4, 127.8, 127.3, 126.5, 90.0, 26.0; HPLC method A (gradient; ACN/H₂O 30:70–80:20, 0–20 min, ACN/H₂O 80:20–30:70, 20–40 min; 0.1% TFA): rt = 7.75 min, purity = 97.4%; HPLC method B (isocratic; MeOH/H₂O 50:50, 60 min; 0.1% TFA): rt = 11.05 min, purity = 96.9%.

4.1.19. 5-((3-Chlorophenylthio)methyl)-1H-pyrazol-3(2H)-one (15)

In analogy to **5**, compound **15** was prepared following the general procedure of ASPII products. 3-Chlorobenzenethiol (0.50 g, 3.46 mmol) was treated with ethyl 4-chloroacetoacetate (0.47 mL, 3.46 mmol) and triethylamine (0.72 mL, 5.19 mmol) to afford ethyl 4-(3-chlorophenylthio)-3-oxobutanoate (0.74 g, 2.70 mmol). Immediately after flash column ethyl 4-(3-chlorophenylthio)-3-oxobutanoate (0.74 g, 2.70 mmol) was allowed to react with hydrazine (2 N in EtOH, 1.35 mL, 2.70 mmol) to give **15** as a white solid (0.27 g, 33%, two steps). ¹H NMR (500 MHz, DMSO-*d*₆, δ): 11.60 (br s, 1H), 9.54 (br s, 1H), 7.40–7.22 (m, 4H), 5.33 (s, 1H), 4.13 (s, 2H); ¹³C NMR (125 MHz, DMSO-*d*₆, δ): 160.8, 138.7, 133.6, 130.6, 126.8, 126.3, 125.6, 89.8, 27.0; HPLC method A (gradient; ACN/H₂O 30:70–80:20, 0–20 min, ACN/H₂O 80:20–30:70, 20–40 min; 0.1% TFA): rt = 8.28 min, purity = 95.3%; HPLC method B (isocratic; MeOH/H₂O 50:50, 60 min; 0.1% TFA): rt = 13.67 min, purity = 99.2%.

4.1.20. 5-((2,4-Dichlorophenylthio)methyl)-1H-pyrazol-3(2H)-one (16)

In analogy to **5**, compound **16** was prepared following the general procedure of ASPII products. 2,4-Dichlorobenzenethiol (1.00 g, 5.58 mmol) was treated with ethyl 4-chloroacetoacetate (0.76 mL, 5.58 mmol) and triethylamine (1.16 mL, 8.32 mmol) to afford ethyl 4-(2,4-dichlorophenylthio)-3-oxobutanoate (1.09 g, 3.55 mmol). Immediately after flash column ethyl 4-(2,4-dichlorophenylthio)-3-oxobutanoate (0.59 g, 1.92 mmol) was allowed to react with hydrazine (2 N in EtOH, 0.96 mL, 1.92 mmol) to give **16** as a white solid (0.034 g, 4%, two steps). ¹H NMR (400 MHz, DMSO-*d*₆, δ): 9.92 (br s, 1H), 7.63 (s, 1H), 7.47–7.39 (m, 2H), 5.38 (s, 1H), 4.15 (s, 2H); ¹³C NMR (100 MHz, DMSO-*d*₆, δ): 159.0, 139.4, 134.9, 131.7, 130.3, 128.9, 128.7, 127.8, 89.3, 27.1; HPLC method A (gradient; ACN/H₂O 30:70–80:20, 0–20 min, ACN/H₂O 80:20–30:70, 20–40 min; 0.1% TFA): rt = 10.52 min, purity = 99.0%; HPLC method B (isocratic; MeOH/H₂O 60:40, 60 min; 0.1% TFA): rt = 10.73 min, purity = 98.7%.

4.1.21. 5-((3,4-Dichlorophenylthio)methyl)-1H-pyrazol-3(2H)-one (17)

In analogy to **5**, compound **17** was prepared following the general procedure of ASPII products. 3,4-Dichlorobenzenethiol (1.00 g, 5.58 mmol) was treated with ethyl 4-chloroacetoacetate (0.76 mL, 5.58 mmol) and triethylamine (1.16 mL, 8.32 mmol) to afford ethyl 4-(3,4-dichlorophenylthio)-3-oxobutanoate (1.67 g, 5.44 mmol). Immediately after flash column ethyl 4-(3,4-dichlorophenylthio)-3-oxobutanoate (1.13 g, 3.68 mmol) was allowed to react with hydrazine (2 N in EtOH, 1.83 mL, 3.66 mmol) to give **17** as a white solid (0.67 g, 64%, two steps). ¹H NMR (400 MHz, DMSO-*d*₆, δ): 10.66 (br s, 1H), 7.59 (s, 1H), 7.52 (d, *J* = 8.4 Hz, 1H), 7.30 (d, *J* = 8.0 Hz, 1H), 5.34 (s, 1H), 4.14 (s, 2H); ¹³C NMR (125 MHz, DMSO-*d*₆, δ): 159.5, 140.6, 137.3, 131.5, 130.7, 129.0, 128.2, 128.0, 88.8, 27.8; HPLC method A (gradient; ACN/H₂O 30:70–80:20, 0–20 min, ACN/H₂O 80:20–30:70, 20–40 min; 0.1% TFA): rt = 10.47 min, purity = 99.5%; HPLC method B (isocratic; MeOH/H₂O 60:40, 60 min; 0.1% TFA): rt = 11.17 min, purity = 95.6%.

4.1.22. 5-((2,6-Dichlorophenylthio)methyl)-1H-pyrazol-3(2H)-one (18)

In analogy to **5**, compound **18** was prepared following the general procedure of ASPII products. 2,6-Dichlorobenzenethiol (1.00 g, 5.58 mmol) was treated with ethyl 4-chloroacetoacetate (0.76 mL, 5.58 mmol) and triethylamine (1.16 mL, 8.32 mmol) to afford ethyl 4-(2,6-dichlorophenylthio)-3-oxobutanoate (1.72 g, 5.58 mmol). Immediately after flash column ethyl 4-(2,6-dichlorophenylthio)-3-oxobutanoate (1.72 g, 5.58 mmol) was allowed to react with hydrazine (2 N in EtOH, 2.80 mL, 5.60 mmol) to give **18** as a white solid (0.34 g, 22%, two steps). ¹H NMR (500 MHz, DMSO-*d*₆, δ): 11.45 (br s, 1H), 9.35 (br s, 1H), 7.55 (d, *J* = 8.5 Hz, 2H), 7.38 (t, *J* = 8.0 Hz, 1H), 5.12 (s, 1H), 4.01 (s, 2H); ¹³C NMR (125 MHz, DMSO-*d*₆, δ): 161.1, 140.5, 131.3, 138.4, 129.0, 89.5, 28.9; HPLC method A (gradient; ACN/H₂O 30:70–80:20, 0–20 min, ACN/H₂O 80:20–30:70, 20–40 min; 0.1% TFA): rt = 8.22 min, purity = 96.0%; HPLC method B (isocratic; MeOH/H₂O 50:50, 60 min; 0.1% TFA): rt = 14.33 min, purity = 98.2%.

4.1.23. 5-((3,5-Dichlorophenylthio)methyl)-1H-pyrazol-3(2H)-one (19)

In analogy to **5**, compound **19** was prepared following the general procedure of ASPII products. 3,5-Dichlorobenzenethiol (5.00 g, 27.9 mmol) was treated with ethyl 4-chloroacetoacetate (3.80 mL, 27.9 mmol) and triethylamine (6.00 mL, 43.0 mmol) to afford ethyl 4-(3,5-dichlorophenylthio)-3-oxobutanoate (8.40 g, 27.3 mmol). Immediately after flash column ethyl 4-(3,5-dichlorophenylthio)-3-oxobutanoate (4.09 g, 13.3 mmol) was allowed to react with hydrazine (2 N in EtOH, 6.70 mL, 13.4 mmol) to give **19** as a white solid (2.63 g, 71%, two steps). ¹H NMR (500 MHz, DMSO-*d*₆, δ): 11.57 (br s, 1H), 9.44 (br s, 1H), 7.39 (s, 3H), 5.34 (s, 1H), 4.18 (s, 2H); ¹³C NMR (125 MHz, DMSO-*d*₆, δ): 159.1, 140.9, 134.4, 125.4, 125.1, 88.6, 27.6; HPLC method A (gradient; ACN/H₂O 30:70–80:20, 0–20 min, ACN/H₂O 80:20–30:70, 20–40 min; 0.1% TFA): rt = 10.70 min, purity = 98.4%; HPLC method B (isocratic; MeOH/H₂O 60:40, 60 min; 0.1% TFA): rt = 13.73 min, purity = 97.9%.

4.2. In vitro pharmacokinetic studies of 1

All of these studies were performed at Apredica, Inc. in Watertown, MA.

4.2.1. Chromatography and mass spectrometry

Samples were analyzed by LC–MS/MS using an Agilent 6410 mass spectrometer coupled with an Agilent 1200 HPLC and a CTC PAL chilled auto sampler, all controlled by MassHunter software (Agilent). After separation on a C18 reverse phase HPLC column (Agilent, Waters, or equivalent) using a 4 min acetonitrile–water gradient system, peaks were analyzed by mass spectrometry (MS) using ESI ionization in the MRM mode. The mass spectrometer gas flows and voltages were individually tuned to provide optimal signal for each compound. Trial spectra were obtained to determine the best conditions for data collection. The transition(s) that gave the best signal/noise ratio were used for data analysis. See [Supplementary data](#) for representative MS spectra and chromatography data.

4.2.2. Microsomal stability

Test compounds were incubated in duplicate at 5 μM concentration with human or mouse microsomes at 37 °C. The reaction mixture contained 0.275 mg/mL microsomal protein in 100 mM potassium phosphate, 2 mM NADPH, 3 mM MgCl₂, pH 7.4. A control was run for each test agent omitting NADPH to detect NADPH-independent degradation. After 15 s, 10 min, 20 min, 40 min, and 60 min incubation, aliquots were removed from each

experimental and control reaction and mixed with an equal volume of ice-cold Stop Solution (0.3% acetic acid in acetonitrile containing 0.3 μM haloperidol as an internal standard). Stopped reactions were incubated at least 10 min at -20°C , and an additional volume of water was added. The samples were centrifuged to remove precipitated protein, and the supernatants were analyzed by LC–MS/MS to quantify the remaining parent. Excel was used for the calculations. The response ratio (RR) was calculated by the Mass Hunter software by dividing the peak area of the analyte by the peak area of the internal standard. The relative ratio was calculated by dividing the RR with NADPH by the RR from the $-$ NADPH control at the same time point.

$$(\text{Relative ratio} = \text{PA}_{+\text{NADPH}}/\text{PA}_{-\text{NADPH}})$$

The % remaining (RE) compound was calculated by dividing the relative ratio of the sample in question by A_0 ,

$$\text{RE} = \text{RR}/A_0$$

where A_0 is a correction factor for small differences in the starting concentration, extraction efficiency, etc. Curve fitting was used to determine A_0 , k (first-order rate constant) using an exponential fit with $1/Y$ weighting. The half-life was calculated as: $T_{1/2} = \ln(2)/k$. The intrinsic clearance was calculated as follows: $\text{CL}'_{\text{int}} = (0.693/T_{1/2}) \times (\text{mL incubation}/\text{mg microsomal protein}) \times (\text{mg microsomal protein}/\text{g liver}) \times (\text{g liver}/\text{kg bodyweight})$.²⁹ The scale-up factor for microsomes protein to g of liver is 45 mg/g of liver.³⁰ Liver weights used for human and mice were 20 g/kg body weight and 34 g/kg body weight, respectively.^{31,32} The units on the CL'_{int} are mL/min/kg. See [Supplementary data](#) for human/mouse microsomal stability of **1**, **2**, and other ASP compounds.

4.2.3. Caco-2 monolayer permeability

Caco-2 permeability is measured by detecting the amount of compound that permeates through a confluent monolayer of Caco-2 cells. Caco-2 cells grown in tissue culture flasks were trypsinized, suspended in medium, and the suspensions were applied to wells of a collagen-coated BioCoat Cell Environment in a 24-well format (BD Biosciences). The cells were allowed to grow and differentiate for three weeks, feeding at 2-day intervals.

Stock solutions of 10 mM test compound or control prepared in DMSO were used to prepare solutions for the Caco-2 permeability studies. For apical to basolateral (A \rightarrow B), the apical (A-side) buffer contained 50 μM test compound or control and 100 μM Lucifer yellow dye in the transport buffer (1.98 g/L glucose in 10 mM HEPES, 1 \times Hank's Balanced Salt Solution) at pH 6.5; the basolateral (B-side) buffer was the transport buffer at pH 7.4. For B \rightarrow A studies, the A-side buffer contained 100 μM Lucifer yellow in the transport buffer, pH 6.5, and the B-side buffer contained 50 μM test compound or control in the transport buffer, pH 7.4. The Caco-2 cells were incubated with these buffers for 2 h, and the cell buffers and dosing solutions were removed for analysis.

To verify that the Caco-2 cell monolayer was properly formed, an aliquot of the cell buffer from each well was analyzed by fluorescence to determine the transport of the impermeable dye Lucifer Yellow. In all cases, acceptable transport of Lucifer Yellow was observed (<1% transport in 2 h).

Caco-2 results are reported as apparent permeability, P_{app} , expressed in units of 10^{-6} cm/s:

$$P_{\text{app}} = \frac{dQ/dt}{c_0 A}$$

where dQ/dt is the rate of permeation (mol test compound transported per unit time), c_0 is the initial concentration of test

compound, and A is the area of the cell monolayer. See [Supplementary data](#) for Caco-2 permeability of **1** and other compounds.

4.2.4. Solubility screen

The solubility of the test compounds in PBS was estimated by absorbance. Threefold serial dilutions were prepared in DMSO at 100 times the final concentration. This DMSO stock was diluted to the final concentration in PBS, the plate was incubated at room temperature for 1 h, then it was examined visually for the formation of precipitate, and the absorbance at 450 nm was measured. For non-colored compounds, the absorbance value was used to detect solubility, while for highly colored compounds, visual inspection was used. The highest concentration that was not visibly cloudy and whose absorbance was not different from background was judged to be the solubility limit (see [Supplementary data](#)).

4.2.5. Plasma and PBS stability

The test compounds, with warfarin and diltiazem as controls, were incubated in mouse plasma and phosphate buffered saline in duplicate at 5 μM . The time-zero samples were taken immediately (15 s) after adding the compounds. The plate containing the plasma and PBS samples was incubated at 37°C , and then time points were taken at 10, 20, 40, 60 min in the same way. The plasma samples and PBS samples were precipitated with acetonitrile containing haloperidol as an internal standard and either centrifuged or filtered through a Varian Captiva plate (following the manufacturer's directions) to remove precipitated protein. The samples were then analyzed on LC–MS/MS.

The response ratio (RR = area of analyte peak divided by the area of the internal standard peak), as calculated by the LC–MS software, was used for determining the plasma stability. The relative ratio was calculated by dividing the RR from plasma by the RR from the PBS control at the same time point.

$$(\text{Relative ratio} = \text{RR}_{\text{plasma}}/\text{RR}_{\text{PBS}})$$

The % remaining (RE) compound was calculated by dividing the relative ratio of the sample in question by A_0 ,

$$\text{RE} = \text{RR}/A_0$$

where A_0 is a correction factor for small differences in starting concentration, extraction efficiency, etc. Curve fitting was used to determine A_0 , k (first-order rate constant) using an exponential fit with $1/Y$ weighting. The half-life was calculated as: $T_{1/2} = \ln(2)/k$.

To determine PBS half-life, the RR was fit to a first-order exponential curve to determine A_{PBS} and k_{PBS} : $\text{RR} = A_{\text{PBS}}e^{-k_{\text{PBS}}t}$. The half-life was calculated as above: $T_{1/2} = \ln(2)/k_{\text{PBS}}$. See [Supplementary data](#) for mouse plasma stability of **1**.

4.3. Brain uptake study of compound 2

4.3.1. General methods and materials

Bioanalytical HPLC analyses were determined on a Dionex HPLC system (Dionex, Sunnyvale, CA) using a Phenomenex (Torrance, CA) Luna C18 column (250 \times 2.0 mm, 5 μM) and guard column with a flow rate of 0.2 mL/min. The mobile phase used in HPLC consisted of 0.1% (v/v) formic acid (Fluka) in water as solvent A and 80% acetonitrile (Fluka), 0.08% formic acid in water as solvent B. All water used was Milli-Q water obtained using a Biocel A10 water purification system from Millipore Corporation (Bedford, MA). Solid phase extraction (SPE) was carried out using Waters Sep-Pak[®] Vac C18 1cc cartridges (Waters Chromatography, Milford, MA). Analysis of biological samples was carried out using an API 3000 liquid chromatography–tandem mass spectrometry system (Applied biosystems, Foster city, CA) equipped with an Agilent 1100 series HPLC system (Agilent Technologies, Wilmington, DE).

Sample concentration was performed in a Genevac EZ-2^{plus} (Genevac Inc., Valley Cottage, NY).

4.3.2. Preparation of plasma standard curve

Samples were prepared in $\mu\text{g}/\text{mL}$ stock solutions to obtain final concentrations in $\mu\text{g}/\text{mL}$. A typical standard curve contained the concentrations 0.01, 0.05, 0.1 and 0.5 $\mu\text{g}/\text{mL}$ of **2** in human serum. To an aliquot of the sample (100 μL) was added **1** (internal standard, 10 μL of 50 $\mu\text{g}/\text{mL}$). The solvent was removed under a stream of nitrogen and the residue was reconstituted in LC–MS/MS mobile phase (200 μL , reconstitution condition 66.66% H_2O and 33.3% acetonitrile). An aliquot (20 μL) was analyzed by LC–MS. Standards were run in triplicate. See [Supplementary data](#) for plasma standard curve of **2**.

4.3.3. Preparation of brain standard curve

To a homogenizer was added **2** (50 or 100 μL of an aqueous solution from different concentrated stock solutions), acetonitrile (650 or 600 μL), **1** (internal standard, 10 μL of 50 $\mu\text{g}/\text{mL}$ stock solution) and a piece of pig brain weighing between 300 and 500 mg. The compound of interest was added to obtain a final concentration in $\mu\text{g}/\text{mL}$ based on a total volume of 1 mL. A typical standard curve would contain the concentrations 0.05, 0.10, 0.5 and 1.0 $\mu\text{g}/\text{mL}$. The brain was homogenized and transferred to a centrifuge tube. The homogenizer was washed with acetonitrile (300 μL), which was also added to the centrifuge tube. The samples were centrifuged (10 krpm, 12 min), and the supernatant was transferred to a separate tube. An aliquot (400 μL) was loaded onto a Waters Sep-Pak[®]Vac C18 1cc SPE column. The SPE column was washed with 10% acetonitrile and 90% H_2O ($2 \times 400 \mu\text{L}$), and the compounds were eluted ($2 \times 1 \text{ mL}$). The solvent was removed under a stream of nitrogen, and the residue was reconstituted in the LC–MS/MS mobile phase (200 μL , reconstitution solvent 66.66% H_2O and 33.3% acetonitrile). An aliquot (20 μL) was analyzed by LC–MS/MS. Standards were run in triplicate. See [Supplementary data](#) for brain standard curve of **2**.

4.3.4. Administration of compound 2 to mice

Compound **2** was diluted in 60% PBS and 40% DMSO to form a stock solution. Three mice (#1–#3, female, Tg6799 colony with B6/SJL background) were weighed and then given the compound (100 μL per 10 g, final dose 1 mg/kg) via intraperitoneal injection and sacrificed 10 min after compound administration. Mouse #4 did not receive any drug and was sacrificed to be used as blank. The mice were anesthetized with pentobarbital (100 μL of a 50 mg/mL solution in PBS) before the desired time of sacrifice. Once the animal was no longer responsive, its thoracic cavity was opened, and blood was removed from the right ventricle of the heart using a syringe that had been treated with heparin and transferred to Microtainer PST pre-heparinized tubes. The tubes were centrifuged (5 min at 6 krpm), and the plasma supernatants were transferred to labeled tubes. The brain was perfused with PBS by inserting a needle through the left ventricle and allowing PBS under pressure to flow into it. The right atrium was cut to relieve the pressure. The mouse was decapitated, and the brain was removed. All samples were flash-frozen in liquid nitrogen and stored at -20°C until analyzed.

4.3.5. Preparation of plasma samples for quantification

To an aliquot of the sample was added **1** (internal standard, 10 μL of 50 $\mu\text{g}/\text{mL}$). The solvent was removed under a stream of nitrogen, and the residue was reconstituted in the LC–MS/MS mobile phase (200 μL , reconstitution solvent 66.66% H_2O and 33.3% acetonitrile). An aliquot (20 μL) was analyzed by LC–MS/MS.

Quantification of the compounds was carried out by calculating the ratio of the mass spectral peak intensity of the internal standard and comparing it to the standard curve. The data were originally obtained in $\mu\text{g}/\text{mL}$, but were converted to μM for ease of comparison.

4.3.6. Preparation of brain samples for quantification

Brains were thawed and weighed. The brain was added to a homogenizer with acetonitrile (700 μL) and **1** (internal standard, 10 μL of 50 $\mu\text{g}/\text{mL}$). The brain was homogenized and transferred to a centrifuge tube. The homogenizer was washed with acetonitrile (300 μL), which was also added to the centrifuge tube. The samples were centrifuged (10 krpm, 12 min), and the supernatant was transferred to a separate tube. An aliquot (400 μL) was loaded onto a Waters Sep-Pak[®]Vac C18 1cc SPE column. The SPE column was washed with 10% acetonitrile and 90% H_2O ($2 \times 400 \mu\text{L}$), and the compounds were eluted ($2 \times 1 \text{ mL}$). The solvent was removed under a stream of nitrogen, and the residue was reconstituted in the LC–MS/MS mobile phase (200 μL , reconstitution solvent 66.66% H_2O and 33.3% acetonitrile). An aliquot (20 μL) was analyzed by LC–MS/MS. Quantification of the compound was carried out by calculating the ratio of the peak intensity of the compound to the peak intensity of the internal standard and comparing it to the standard curve. The final value in $\mu\text{g}/\text{mL}$ was divided by the mass of the brain to obtain a concentration in μg of compound/g of brain. For display on the charts, this was converted to a concentration in μM by assuming that the density of the brain tissue is approximately 1 g/mL.

4.3.7. Brain/plasma ratio of the experimental mice

See [Supplementary data](#) for data.

4.4. Determination of EC₅₀ values and viability

These experiments are described in the previous paper.¹²

Acknowledgments

We thank the National Institutes of Health [1R43NS057849], the ALS Association (TREAT program), the Department of Defense [AL093052] and the Veterans Administration at the Edith Nourse Rogers Memorial Veterans Hospital, Bedford, MA for their generous support of the research project. The authors are grateful to Dr. Michael Avram and Lynn Luong of the Northwestern University Clinical Pharmacology Core Facility and the Pharmaceutical Chemistry Translational Resource of the Center for Molecular Innovation and Drug Discovery for carrying out the LC–MS experiments for the blood–brain barrier penetration studies. Representative HTS hit compounds of ASP scaffold, data from in vitro ADME assays for ASP compounds, and the brain uptake study for compound **2** are available.

Supplementary data

Supplementary data associated with this article can be found, in the online version, at [doi:10.1016/j.bmc.2010.10.052](https://doi.org/10.1016/j.bmc.2010.10.052).

References and notes

1. Bruijn, L. I.; Miller, T. M.; Cleveland, D. W. *Annu. Rev. Neurosci.* **2004**, *27*, 723.
2. Hirtz, D.; Thurman, D. J.; Gwinn-Hardy, K.; Mohamed, M.; Chaudhuri, A. R.; Zalutsky, R. *Neurology* **2007**, *68*, 326.
3. Cronin, S.; Hardiman, O.; Traynor, B. J. *Neurology* **2007**, *68*, 1002.
4. Rowland, L. P.; Shneider, N. A. *N. Eng. J. Med.* **2001**, *344*, 1688.
5. Miller, R. G.; Mitchell, J. D.; Moore, D. H. *ALS Other Motor Neuron Disord.* **2003**, *4*, 191.
6. Gros-Louis, F.; Gaspar, C.; Rouleau, G. A. *Biochim. Biophys. Acta* **2006**, *1762*, 956.

7. Rosen, D. R.; Siddique, T.; Patterson, D.; Figlewicz, D. A.; Sapp, P.; Hentati, A.; Donaldson, D.; Goto, J.; O'Regan, J. P.; Deng, H.; Rahmani, Z.; Krizus, A.; Mckenna-Yasek, D.; Cayabyab, A.; Gaston, S. M.; Berger, R.; Tanzi, R. E.; Halperin, J. J.; Herzfeldt, B.; Van den Bergh, R.; Hung, W.; Bird, T.; Deng, G.; Mulder, D. W.; Smyth, C.; Laing, N. G.; Soriano, E.; Pericak-Vance, M. A.; haines, J.; Rouleau, G. A.; Gusella, J.; Horvitz, H. R.; Brown, R. H., Jr. *Nature* **1993**, *362*, 59.
8. Bruijn, L. I.; Houseweart, M. K.; Kato, S.; Anderson, K. L.; Anderson, S. D.; Ohama, E.; Reaume, A. G.; Scott, R. W.; Cleveland, D. W. *Science* **1998**, *281*, 1851.
9. Neumann, M.; Sampathu, D. H.; Kwong, L. K.; Truax, A. C.; Micsenyi, M. C.; Chou, T. T.; Bruce, J.; Schuck, T.; Grossman, M.; Clark, C. M.; McCluskey, L. F.; Miller, B. L.; Masliah, E.; Mackenzie, I. R.; Feldman, H.; Feiden, W.; Kretschmar, H. A.; Trojanowski, J. Q.; Lee, V. H. *Science* **2006**, *314*, 130.
10. Kwiatkowski, T. J.; Bosco, D. A.; Leclerc, A. L.; Tamrazin, E.; Vanderburg, C. R.; Russ, C.; Davis, A.; Gilchrist, J.; Kasarskis, E. J.; Munsat, T.; Valdmanis, P.; Rouleau, G. A.; Hosler, B. A.; Cortelli, P.; de Jong, P. J.; Yoshinaga, Y.; Haines, J. L.; Pericak-Vance, M. A.; Yan, J.; Ticozzi, N.; Siddique, T.; Mckenna-Yasek, D.; Sapp, P. C.; Hritz, H. R.; Lanas, J. E.; Brown, R. H., Jr. *Science* **2010**, *323*, 1025.
11. Matsumoto, G.; Stojanovic, A.; Holmber, C. I.; Kim, S.; Morimoto, R. I. *J. Cell Biol.* **2005**, *171*, 75.
12. Benmohamed, R.; Arvanites, A. C.; Kim, J.; Ferrante, R. J.; Silverman, R. B.; Morimoto, R. I.; Kirsch, D. R. *Amotroph. Lat. Scler.* **2010**, *11* in press. doi:10.3109/17482968.2010.522586.
13. Kola, L.; Landis, J. *Nat. Rev. Drug Disc.* **2004**, *3*, 711.
14. Kubinyi, H. *Nat. Rev. Drug Disc.* **2003**, *2*, 665.
15. Tsaïoun, K.; Bottlaender, M.; Mabondzo, A. *BMC Neurol.* **2009**, *9*, S1.
16. Parridge, W. M. *Drug Discovery Today* **2001**, *6*, 1.
17. Hurko, O.; Rayn, J. L. *NeuroRx* **2005**, *2*, 671.
18. Wing, L. K.; Behanna, H. A.; Van Eldik, L. J.; Watterson, M. D.; Ranaivo, H. R. *Curr. Alzheimer Res.* **2006**, *3*, 205.
19. Zimmer, H.; Hillstron, W. W.; Schmidt, J. C.; Seemuth, P. D.; Vogeli, R. *J. Org. Chem.* **1978**, *43*, 1541.
20. Schmidt, D. G.; Zimmer, H. *J. Org. Chem.* **1983**, *48*, 4367.
21. Shimada, K.; Kaburagi, Y.; Fukuyama, T. *J. Am. Chem. Soc.* **2003**, *125*, 4048.
22. Nakajima, T.; Wang, R.; Elovaara, E.; Gonzalez, F. J.; Gelboin, H. V.; Raunio, H.; Pelkonen, O.; Vainio, H.; Aoyama, T. *Biochem. Pharmacol.* **1997**, *53*, 271.
23. Kerns, E. H.; Di, L. *Drug-like Properties: Concepts, Structure, Design, and Methods*; Academic Press, 2009. Chapter 7, p 65.
24. Kerns, E. H.; Di, L. *Drug-like Properties: Concepts, Structure, Design, and Methods*; Academic Press, 2009. Chapter 26, p 291.
25. Balimane, P. V.; Han, Y.; Chong, S. *AAPS J.* **2006**, *8*, 1.
26. Kerns, E. H.; Di, L. *Drug-like Properties: Concepts, Structure, Design, and Methods*; Academic Press, 2009. p 161, Chapter 11.
27. Silverman, R. B.; Lawton, G. R.; Ranaivo, H. R.; Chico, L. K.; Seo, J.; Watterson, D. M. *Bioorg. Med. Chem.* **2009**, *17*, 7593.
28. Lawton, G. R.; Ranaivo, H. R.; Chico, L. K.; Ji, H.; Xue, F.; Martasek, P.; Roman, L. J.; Watterson, D. M.; Silverman, R. B. *Bioorg. Med. Chem.* **2009**, *17*, 2371.
29. Obach, R. S. *Drug Metab. Dispos.* **1999**, *27*, 1360–1359.
30. Houston, J. B. *Biochem. Pharmacol.* **1994**, *47*, 1469.
31. Obach, R. S.; Baxter, J. G.; Liston, T. E.; Silber, B. M.; Jones, B. C.; MacIntyre, R.; Rance, D. J.; Wastall, P. *J. Pharmacol. Exp. Ther.* **1997**, *283*, 46.
32. Brown, R. P.; Delp, M. D.; Lindstedt, S. L.; Rhomberg, L. R.; Belile, R. P. *Toxicol. Ind. Health* **1997**, *13*, 407.